Pflugers Arch - Eur J Physiol (2008) 456:139–153
DOI 10.1007/s00424-007-0431-z

INVITED REVIEW

Nuclear architecture and chromatin dynamics revealed by atomic force microscopy in combination with biochemistry and cell biology

Yasuhiro Hirano · Hirohide Takahashi · Masahiro Kumeta · Kohji Hizume · Yuya Hirai · Shotaro Otsuka · Shige H. Yoshimura · Kunio Takeyasu

Received: 1 October 2007 / Revised: 29 November 2007 / Accepted: 10 December 2007 / Published online: 3 January 2008
© Springer-Verlag 2007

Abstract The recent technical development of atomic force microscopy (AFM) has made nano-biology of the nucleus an attractive and promising field. In this paper, we will review our current understanding of nuclear architecture and dynamics from the structural point of view. Especially, special emphases will be given to: (1) How to approach the nuclear architectures by means of new techniques using AFM, (2) the importance of the physical property of DNA in the construction of the higher-order structures, (3) the significance and implication of the linker and core histones and the nuclear matrix/scaffold proteins for the chromatin dynamics, (4) the nuclear proteins that contribute to the formation of the inner nuclear architecture. Spatio-temporal analyses using AFM, in combination with biochemical and cell biological approaches, will play important roles in the nano-biology of the nucleus, as most of nuclear structures and events occur in nanometer, piconewton and millisecond order. The new applications of AFM, such as recognition imaging, fast-scanning imaging, and a variety of modified cantilevers, are expected to be powerful techniques to reveal the nanostructure of the nucleus.

Keywords Human · Cultured cells · Transport · *Xenopus laevis* · Regulation

Y. Hirano · H. Takahashi · M. Kumeta · K. Hizume · Y. Hirai · S. Otsuka · S. H. Yoshimura · K. Takeyasu (✉)
Kyoto University Graduate School of Biostudies,
Yoshida-Honmachi, Sakyo-ku,
Kyoto 606-8501, Japan
e-mail: takeyasu@lif.kyoto-u.ac.jp

Architecture and biological significance of the nucleus: an overview

The nucleus is the biggest organelle in eukaryotic cells (10–20 μm in a diameter in mammalian cells), and it packages the entire genome. It has long been thought that the nucleus is a container that holds nuclear events including gene duplication, transcription, and damage repair. Recent reports, however, have shown that the architecture of the nucleus itself plays important roles in the regulation of genome functions and structures. Namely, the nuclear architecture is closely related to the nuclear functions [1, 2].

In eukaryotes, the genomic DNA is separated from the cytoplasm by the nuclear envelope and forms chromatin inside the nucleus [3–6]. Chromatin formation is achieved through several DNA-folding steps. First, 146-bp DNA segments wrap around a histone octamer (two each of H2A, H2B, H3, and H4) in 1.65 turns to form a nucleosome [7]. The linker histones, which include H1, H5, and other subtypes, are major components of the chromatin and play a significant role in the higher-order packaging of the array of nucleosomes called the "beads-on-a-string" fiber to form the 30-nm fiber [8–11]. In addition to the linker histones, non-histone proteins, such as high mobility group proteins, condensins, and topoisomerases, are also involved in the higher-order structure of the chromatin [12]. In particular, the condensin complex and topoisomerase II (Topo II) are thought to hold two DNA strands in remote regions to create tension in the trapped DNA region [13, 14]. The higher-order chromatin forms transcriptional active and inactive regions named euchromatin and heterochromatin, respectively [15].

A well-known function of the nuclear envelope is protection of the genome from environmental damage, such

as ultraviolet irradiation. Moreover, the nuclear envelope also plays other important roles including nuclear transport and regulation of chromatin functions. The nuclear envelope is composed of double lipid bilayers [16] (an outer and an inner nuclear membrane; ONM and INM, respectively), the nuclear pore complex (NPC), and the nuclear lamina. Heterochromatin attaches to both the INM and the nuclear lamina (for a detailed description of the nuclear envelope, see reviews [17–20]). It is thought that the ONM and the endoplasmic reticulum (ER) are the same compartment, as the ONM continues from the ER and ribosomes exist on the ONM. On the other hand, the INM contains specific INM proteins, such as the lamin B receptor (LBR) [21, 22], lamina-associated polypeptides [23], emerin [24], MAN1 [25], and the SUN proteins [26, 27]. Recent proteomic analysis has revealed that about 80 proteins exist in the INM [28]. Some of the INM proteins interact with chromatin and/or the nuclear lamina [26, 29] (see "Interaction between the nuclear envelope and chromatin").

The inside of the nucleus can be roughly divided into two regions: chromosome territory and the interchromatin compartment. The chromosome territory is the region that is occupied by chromatin. Heterochromatin is located under the nuclear envelope, around the nucleolus, and in the inner region of the chromatin territory, whereas euchromatin with transcriptional activities is situated at the boundary between the chromatin territory and the interchromatin compartment [30, 31]. The interchromatin compartment seems to exclude chromatin and contains sub-compartments including the nuclear matrix, nuclear speckle, Cajal body, promyelocytic leukemia (PML) body, and nucleolus (see "Inner-nuclear structures that interact with chromatin"). These sub-compartments function as the scaffolds for ribosome biogenesis [32], RNA maturation, and other processes. In the interchromatin region, proteins and RNA cooperate to promote biological activities such as transcription and RNA splicing under a constant cycle of assembly and disassembly.

The nucleus possesses a highly complex but well-organized architecture, and the dynamic functions of the nucleus depend on this architecture. Thus, it is important to elucidate the molecular mechanisms of individual nuclear events in relation to specific nuclear structures, hopefully at the nanometer, millisecond, and piconewton levels. Due to the complexity of such nuclear events, the elucidation of the mechanisms will require a coordinated combination of techniques in nanotechnology, biochemistry, and cell and molecular biology.

New approaches to studies of nuclear architecture

The recent development of atomic force microscopy (AFM) [33] has been a breakthrough in the study of nuclear architecture [16, 34, 35]. The instrumentation and application of AFM have been enormously fruitful due to the development of sharp cantilevers for molecular imaging [36–38], cantilever modification techniques for single-molecule force measurement [39–43], and fast-scanning devices for real-time imaging [44–48].

Nanometer scale imaging by AFM

AFM scans the sample surface with a very sharp probe and reveals the surface topography [34, 49, 50]. Thus, AFM routinely identifies the binding site of a DNA-binding protein with a resolution of several tens of base pairs and determines the degree of protein polymerization on a liner DNA of several kilobase pairs [51]. AFM has also revealed the distinct higher-order structures of DNA, including supercoiling [52], stem-loop structures [53], and enhancer-promoted DNA loops [54] as well as nucleosomes and chromatins [55].

The sequential removal of the cell membranes, cytoplasm, and nucleoplasm from cultured cells on a cover slip (Fig. 1a and b) leads to the exposure of interphase chromatin [56]. By using this method and nanoscale imaging, the inner chromatin structures inside the interphase nucleus have been revealed (Fig. 1c and d) [57]. The depletion of cytoplasmic and nucleoplasmic materials from HeLa cells exposes the interphase chromosome that is composed of an ~80-nm diameter granular unit that forms an ~80-nm-wide fiber (Fig. 1e and f). In contrast, cytoskeletal fibers are always thinner, with a width of 10–60 nm (Fig. 1g and h).

In human mitotic chromosomes, 70- to 80-nm granular structures become evident under varying concentrations of Mg^{2+} in electron microscopy (EM) [58] and after treatment with RNase and pepsin in AFM [59]. In the mitotic chromosome of *Drosophila melanogaster*, the fibrous structures with ~40 and 80 nm widths can be observed by EM [60]. On the surface of condensed chromosomes purified from sperm cells, ~70-nm particles have also been identified [61]. When the chromosome is dissected with the AFM tip and its internal structures are visualized, ~70-nm particles that form a fibrous structure are revealed [61]. These lines of evidence suggest that the 30- to 40-nm thin fiber and the 70- to 80-nm granular fiber are the fundamental structural units of eukaryotic chromosomes; these fibers are relatively stable in a wide range of experimental conditions. Recent reports have demonstrated that these hierarchical structures exist in both eukaryotes and prokaryotes [35] and that nascent single-stranded RNAs are part of the 30–80 nm fiber structures [62, 63].

Piconewton scale force measurement

Other useful biological applications of AFM are to measure the physical properties of a sample surface and to measure interactive forces between biological macromolecules and

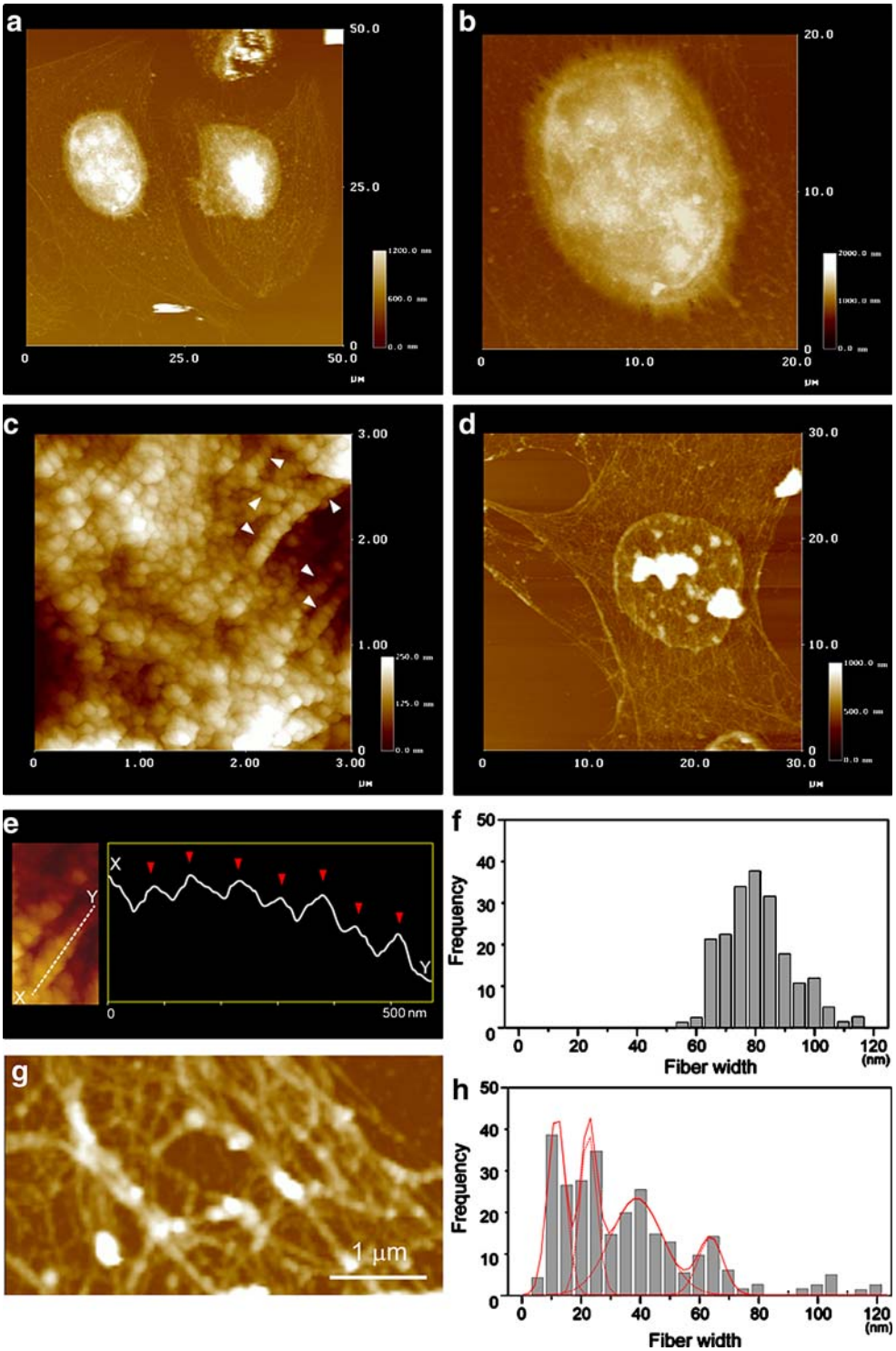

Fig. 1 Micro-dissection of cell nucleus. HeLa cells cultured on a cover glass can be chemically dissected by successive treatment with 0.1% Triton X-100 and 250 mM $(NH_4)_2SO_4$ and 10 U DNase I (**a–c**), followed by 100 U DNase I (**d**). The specimens were then fixed, subjected to a critical-point drying and observed by AFM. Partial treatment with 10 U DNase I exposed chromatin fibers in the nucleus (**c**), whereas the following harsh treatment with 100 U DNase I removed all of these fibers and revealed the nuclear matrix (**d**). **e** Section analysis of the chromatin fiber observed in (**c**) shows granular units (*arrowheads*). **f** The width of the chromatin fiber was measured and summarized after subtracting the effect of the AFM tip curvature. The average value was 78.1 nm. **g** and **h** The widths of the cytoskeletal fibers observed in (**a**) were measured and summarized after subtracting the AFM tip curvature. Most of the fiber widths were distributed between 10 and 70 nm with four major peaks with the center values of 11.6, 22.6, 39.1, and 66.4 nm

even between domains within a molecule ([64–68]; also see "Inner-nuclear structures that interact with chromatin"). When the cantilever pushes the sample surface or pulls up one of two interacting molecules, it deflects upward or downward depending on the force applied to it. The force is proportional to the amount of the deflection as described in the following equation: $F=k\Delta x$, where k and Δx stand for the spring constant of the cantilever and the deflection, respectively. Thus, by measuring the cantilever deflection, interactions between biological molecules can be characterized. The application of single-molecule force measurement is described in "Nuclear envelope in interphase."

The force measurement mode can be used to measure the elasticity of living cells. When an AFM cantilever

approaches and pushes against the cell surface, a large indentation in the cell and the cell surface is usually observed after the probe first contacts the cell surface. This indentation can be plotted against the force and fitted to the Hertz model equation [69] to estimate the Young's modulus that describes the elasticity of the sample. The Young's moduli of the areas over the nucleus (1.8±1.5 kPa) are smaller than those of the cell peripheries (5.1±2.9 kPa). The actin network is responsible for the elasticity of the cell [70]; i.e., the degradation of cellular actin by cytochalasin D leads to a decrease in the measured Young's modulus [71, 72]. Immunostaining of actin filaments in HeLa cells indicated that these filaments mainly exist in the peripheral areas of the cell and that only a few filaments can be seen over the nucleus [73]. Thus, the actin distribution might be one reason why the areas over the nucleus appear to be softer than the peripheral areas. The elasticity measurements have shown that both the plasma membrane and the nuclear envelope are soft enough to absorb a large deformation formed by the AFM probe. Penetration of the plasma membrane and the nuclear envelope are possible when the probe indents the cell membrane far down close to a hard glass surface. These types of experiments will provide useful information for the development of single-cell manipulation techniques.

Chemical modification of the AFM cantilever and recognition imaging

The most important issue to be considered in single-molecule force measurement is how to attach the molecule of interest to the cantilever. Specific interactions between glutathione and glutathione *S*-transferase (GST) or between Ni–NTA (nickel–nitrilotriacetic acid) and $(His)_6$ have been used to attach GST-/$(His)_6$-tagged proteins to the AFM cantilever. Methods to covalently bind glutathione or Ni–NTA to an AFM cantilever via a polyethylene glycol (PEG) linker and to attach GST or $(His)_6$-fused protein to this cantilever have been developed [41, 42] (Fig. 2).

Glutathione contains a cysteine residue in the middle of the tri-peptide (NH_2-Gln-Cys-Gly-COOH). The thiol group of the cysteine residue can react to a maleimide group on the PEG-linked AFM cantilever. The rupture force between glutathione and GST was measured to be ~150 pN [42]. Similarly, Ni–NTA can also be attached to an AFM cantilever via a PEG linker with a rupture force of 150–194 pN against $(His)_6$ [41, 74].

The recent development of recognition imaging under the TREC™ mode has enabled researchers to simultaneously obtain a topographic image and a recognition signal and, thus, to identify a specific molecule within the

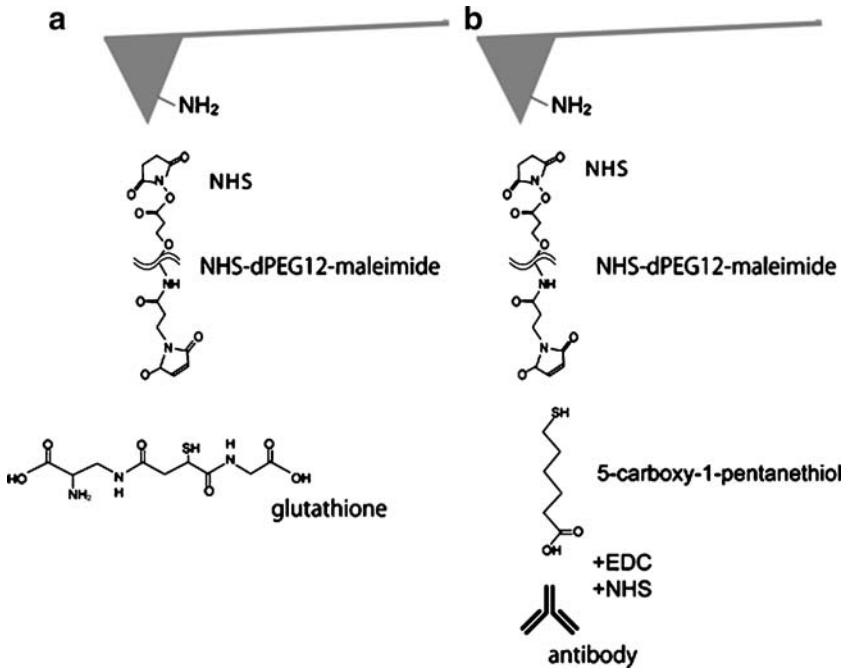

Fig. 2 Chemical modifications to the AFM cantilever. Schematic illustrations of the covalent coupling of glutathione [42] or antibody [115] to an AFM cantilever. The cantilever made of silicon nitride was amino-functionalized by amino-propyl-tetraethoxy-siliane. To avoid steric hindrance from the cantilever surface and to confer enough flexibility, a PEG linker was inserted between the glutathione and the cantilever surface. A hetero-bifunctional PEG linker with N-hydroxysuccinimidyl (NHS) at one end and the maleimide group at the other end was incubated with the functionalized cantilever. Glutathione was then reacted with the PEG-coupled cantilever to covalently attach to the end of PEG (**a**). To attach antibody, 5-carboxy 1-pentanethiol was reacted with the PEG-coupled cantilever. The carboxyl group was activated by EDC and NHS, and then attached to an antibody (**b**)

AFM image. Antibody can also be attached to an AFM cantilever via a PEG linker, and the topographic image and recognition image are obtained simultaneously. With this technique, histone proteins in the reconstituted chromatin have been successfully recognized [75, 76]. The application of TREC™ imaging to the inner nuclear structures is described in "Nuclear matrix."

From nucleosome to chromatin

Physical properties critical for the nucleosomal formation

The first step of genome folding is nucleosome formation, which involves the wrapping of DNA around the core histone octamer. DNA has an elastic property, and physicochemical studies have estimated the persistence length of DNA as 140–180 bp [77–80]. This property of DNA as a stiff polymer largely contributes to the basis of nucleosome maintenance and dynamics. DNA stiffness influences the efficiency of nucleosome formation [81]. The elastic property of DNA also affects the positioning of the histone octamer. Reconstitution with the histone octamer and a short DNA segment (437 bp) has shown a preferential positioning of the core histone at the end of the DNA segment [82] (Fig. 3a).

DNA supercoiling results from DNA winding around DNA-binding proteins and/or from the topological constraint imposed on closed circular DNA. Supercoiling plays important roles in genomic events, such as transcription, replication, and recombination, as well as the maintenance of the genome architecture [83–89].

The superhelical constraint of DNA is a critical determinant of the formation of nucleosomal arrays. When the superhelical constraint is completely removed by topoisomerase I, nucleosomes cannot be formed [90]. The histone-to-DNA-weight ratio during the reconstitution is a critical determinant of the manner of compaction. A large transition between the dense and dispersed states in the reconstituted chromatin depends on the weight ratio. This transition is energetically predicted as a function of the nucleosome–nucleosome distance [91]. These analyses suggest that the interaction between nucleosomes as well as the physical properties of DNA (length and superhelicity) play fundamental roles in chromatin dynamics [16].

Histone H1 converts the "beads-on-a-string" fiber to the 30-nm fiber

Structural and biochemical studies have demonstrated that the linker histone plays a significant role in the higher-order packaging of the "bead-on-a-string" fiber (Fig. 3b). The removal of histone H1 results in the unfolding of the 30-nm fiber to the "beads-on-a-string" fiber [11, 92]. Trypsin digestion of histone H1 and the N terminus of histone H3 leads to a loss of the "zig-zag" arrangement of the nucleosomes and deforms the 30-nm fiber [10]. When purified histone H1 is added to the reconstituted nucleosomes formed on a 100-kbp supercoiled plasmid, the H1-

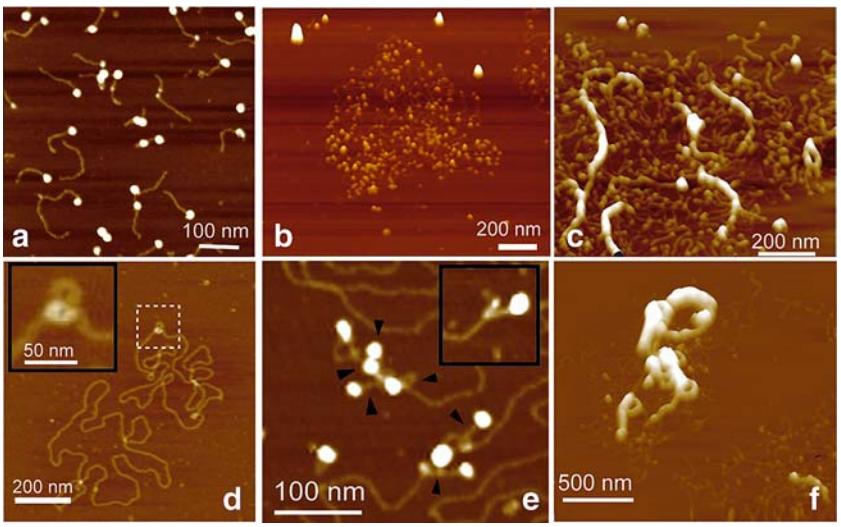

Fig. 3 From DNA to chromatin in vitro. **a** Nucleosomes slide along DNA and tend to stack at the end of DNA [82]. **b** The nucleosome-fiber reconstitution on 100-kbp plasmid in the absence of histone H1. The nucleosome-fiber was reconstituted by a salt dialysis procedure and observed by AFM [8]. **c** The reconstituted chromatin with linker histone H1. Histone H1 was added to the reconstituted nucleosome-fiber after the salt dialysis was completed, and then observed by AFM [8]. **d** Topo II was mixed with 14-kbp plasmid DNA in the absence of ATP and observed by AFM [13]. Topo II forms a homodimer with a ring-like shape. **e** Condensin pentamers were mixed with DNA and subjected to AFM observation [101]. *Arrowheads* indicate condensin–DNA complexes. **f** AFM images of the H1 and Topo II-added chromatin fiber. The H1-added chromatin fiber containing 80 ng DNA was treated with 2 ng of Topo II [13]

containing 30-nm chromatin fibers are formed (Fig. 3c) [8]. These fibers are assumed to be composed of solenoid-like repetitive turns along the fiber axis; namely, they are formed by a three-dimensional arrangement of a nucleosomal array. Several higher-order folding models of the "beads-on-a-string" nucleosomes have been proposed [8, 11, 93]. Because histone H1 reduces the nucleosome–nucleosome distance when it binds to linker DNA [55] and because nucleosomes can freely slide along DNA strands [82], H1 coordinates the assembly of nucleosomes along the DNA strand and contributes to the formation of a well-organized solenoid structure.

Beyond the 30-nm fiber in the nucleus

Topo II and the condensin complex localize to the nuclear matrix fraction of interphase cells [94] and the scaffold fraction of the mitotic chromosome [95]. Topo II forms a ring-shaped homodimer [96, 97] and catalyzes the decatenation and relaxation of the DNA double strand (Fig. 3a) [98]. In *Schizosaccharomyces pombe*, chromosomes cannot be condensed without functional Topo II (Fig. 3d) [99]. The condensin structure maintenance of chromatin (SMC) assumes a head–tail structure, where the head region assembles with non-SMC proteins (Fig. 3e) [100, 101].

When Topo II is added to 30-nm chromatin fibers that have been reconstituted with histone H1, a large complex is formed regardless of the presence of adenosine triphosphate (ATP; Fig. 3f) [13]. This is not the case for the "beads-on-a-string" fibers (i.e., H1-free chromatin fibers). A pull-down assay using GST-H1 also supports this result [13], suggesting that the chromatin compaction by Topo II is not due to a direct interaction between Topo II and histone H1 but rather an interaction between Topo II and H1-containing chromatin regardless of the presence of ATP.

Histone H1 has two possible roles in compaction: (1) It increases the contact area, strengthening the attraction between fibers, and (2) it reduces the negative charge of the nucleosomal complex, decreasing repulsion between fibers. An H1-containing nucleosome has a smaller negative charge (−100 e) than an H1-free nucleosome (−150 e), suggesting that the strength of Coulombic repulsion is smaller when H1 is present. In bulk solution, the H1-induced 30-nm fibers do not aggregate, which suggests that the fibers have a charged colloidal nature [13]. On the other hand, Topo II appears to induce a parallel alignment of double-stranded DNA chains and to promote the formation of thick filaments in the absence of ATP, indicating that Topo II mediates assembly of DNA strands independently of its enzymatic activity. It is assumed that this interaction also occurs within the DNA–histone complex (i.e., nucleosome) in a histone H1-dependent manner. In the absence of H1, each Topo II mediates a weak attraction between the nucleosomes, whereas in the presence of H1, as the contact areas between the fibers are increased, the attraction between two clusters also increases due to the added attraction via Topo II. Therefore, the attraction between 30-nm fibers would be much stronger than the attraction between the pair of nucleosomes, even if Topo II can enhance both attractions.

In the nucleus, chromatin fibers are held by scaffold/matrix structures that occur every several tens or hundreds of kilobases [102], and the matrix-associated region/scaffold associate region (MAR/SAR) forms a complex with many proteins including Topo II [103]. On the other hand, Topo II by itself does not possess a specific affinity for the MAR/SAR sequences and binds directly to any DNA sequence with low affinity [13]. Therefore, in vivo, mechanisms for loading Topo II on the MAR/SAR must exist, and Topo II condenses 30-nm chromatin fibers in concert with other scaffold proteins such as the condensin complex and SAF-A/SP120/hnRNP U (hereafter called as SP120) [104]. A comparison of in vitro and in vivo chromatin structures is required for determining the significance of the MAR/SAR in Topo II-dependent chromatin condensation.

Inner-nuclear structures that interact with chromatin

In addition to the chromosomal compartment, the nucleus contains nonchromosomal compartments such as nucleolus, PML body, nuclear speckle [105], Cajal body [106], and nuclear matrix. Recent studies identified protein components localized in each compartment [107]. Especially, the studies utilizing fluorescence microscopy revealed the localization and dynamics of these proteins in the nucleus [108, 109]. The application of various nano-techniques to the structural and functional analyses of nuclear matrix, nucleolus, and PML body has just become promising in the last 5 years.

Nuclear matrix

In the early 1960s, a non-chromatin internuclear network of ribonucleoproteins with 10-nm branched filaments was identified as the nuclear matrix/scaffold by EM [56, 110, 111]. On the other hand, the nuclear matrix/scaffold was defined biochemically as a remnant structure after a eukaryotic cell is treated with detergent, high salt buffer, and DNase I [112]. It is important to realize that there are no such "insoluble" materials inside the cell nucleus and that the nuclear matrix/scaffold visible under the microscope is the solidified complex formed during chemical treatments [113]. Nevertheless, the nuclear matrix can be observed by AFM. When HeLa cells are gently treated with

Triton X-100, ammonium sulfate, and DNase I, fibrous and dotted structures inside the nucleus are observed (Fig. 5a). Several nuclear proteins have been biochemically identified as the component of the nuclear matrix/scaffold [104]. Among these proteins, the MAR/SAR-binding proteins bind to the MAR/SAR of chromosomal DNA and hold them inside the nucleus.

One of the major MAR-binding proteins, SP120, was identified as one of the heteroribonucleoprotein complexes. This protein has a MAR-binding domain in the N terminus and an arginine–glycine-rich RNA-binding domain in the C terminus [104, 114]. In the nucleus, SP120 interacts and co-localizes with transcriptional factors such as the glucocorticoid receptor and p300 via the RNA-binding domain. In addition, SP120 might interact with several partners (e.g., Topo IIβ) and lead them to different nuclear sub-domains to assure their region-specific localization and function.

Pico-TREC™ can recognize a specific protein by using an antibody-coupled cantilever while obtaining a topographic image with the same probe [75]. The anti-SP120 antibody can be attached to an AFM cantilever with the consumption of less than 10-μg antibody [115], and the localization of SP120 can be elucidated by using this cantilever; individual SP120 molecules can be identified within nuclear components (Fig. 4a–c). This technique will be useful for further structural investigation of the inner-nuclear organization.

PML body

The PML bodies are nuclear matrix-attached particle-like structures that are larger than the nuclear speckles (0.2–1 μm in diameter) and were originally found in PML cells. In the AFM image (Fig. 4d–f), the PML bodies appear as several speckles within the nuclear matrix. One mammalian nucleus has 10–30 PML bodies. The core component of the PML body is a protein called PML, which is a tumor suppressor gene product. Three lysine residues in the PML protein are modified by a ubiquitin-like protein, SUMO-1, and this modification is needed for the formation of PML bodies. The SUMOylation is also essential for PML protein to form a complex with other proteins such as transcription factors (Sp100, CBP), heterochromatin protein HP1, tumor suppressor proteins (Rb, p53), SUMOylation enzymes, and kinases [116–120]. Because of these components, PML bodies are thought to be involved in biological events such as DNA repair, apoptosis, and transcription. In fact, γ-ray irradiation results in the recruitment of p53 to PML, and cells that lack PML fail to induce p53-dependent gene expression [118, 121]. PML bodies could also stabilize transcription co-activator-transcription factor complexes because of their ability to interact with several transcriptional co-activators such as CBP and p300 [122].

Nucleolus

The nucleolus is the most prominent substructure of the nucleus. It is a large assembly of rRNA genes (rDNA), rRNAs, and more than 700 proteins containing RNA transcription factors, processing enzymes, and ribosomal protein subunits [123, 124]. The nucleolus is structurally distinctive among the subcellular organelles because it has no membrane. Nevertheless, there are three different sub-domains in the interphase nucleolus, and each compartment is involved in different steps of ribosomal biogenesis [125, 126]. The fibrillar center (FC) is the center of rRNA transcription and contains the rRNA transcription machinery such as RNA polymerase I and upstream binding factor. The dense fibrillar component (DFC) contains the rRNA early processing factors such as fibrillarin, and the granular component (GC) contains the late processing factors and ribosomal maturation enzymes such as nucleolin and B23 (nucleophosmin). This hierarchical organization of the interphase nucleolus has been shown by EM and fluorescence microscopy; these imaging techniques have revealed that the FC consists of several foci (100–500 nm in diameter) and is surrounded by the DFC [127]. The GC is distributed throughout the whole nucleolus and forms intricate structures with heterochromatin in the periphery [128]. AFM and immunofluorescent microscopy revealed that the nucleolus in HeLa cells is a rigid structure and that it remains on the glass substrate after sequential treatment by detergent, high salt buffer, and DNase I (Fig. 5a, b) [57].

The nucleolus undergoes drastic structural changes during mitosis. The hierarchical structures of the interphase nucleolus collapse in the beginning of mitosis and then gradually reassemble during telophase to early G1 phase. In this mitotic step, nucleolar organizing proteins exhibit distinctive dynamics (Fig. 5c). The FC proteins form foci on chromosome throughout mitosis, and the spots correspond to the nucleolar organizing regions (NORs) on the acrocentric chromosomes as shown by immunostaining on the mitotic chromosome spreads [129]. This mechanism enabled the equal distribution of the proteins into two daughter cells and the resumption of rRNA transcription at telophase. Interestingly, not all NORs are actively transcribed. The active NORs are associated with RNA polymerase I, whereas the inactive NORs contain no transcription machinery and are highly methylated [130]. However, structural differences between these active and inactive chromosomes remain unclear. The recently developed AFM technique of chromosome manipulation and imaging in liquid is expected to soon reveal the nanoscale structure of NORs. The DFC and GC proteins disperse to the cytoplasm in the beginning of mitosis and localize to the surface of condensed chromosomes. During anaphase

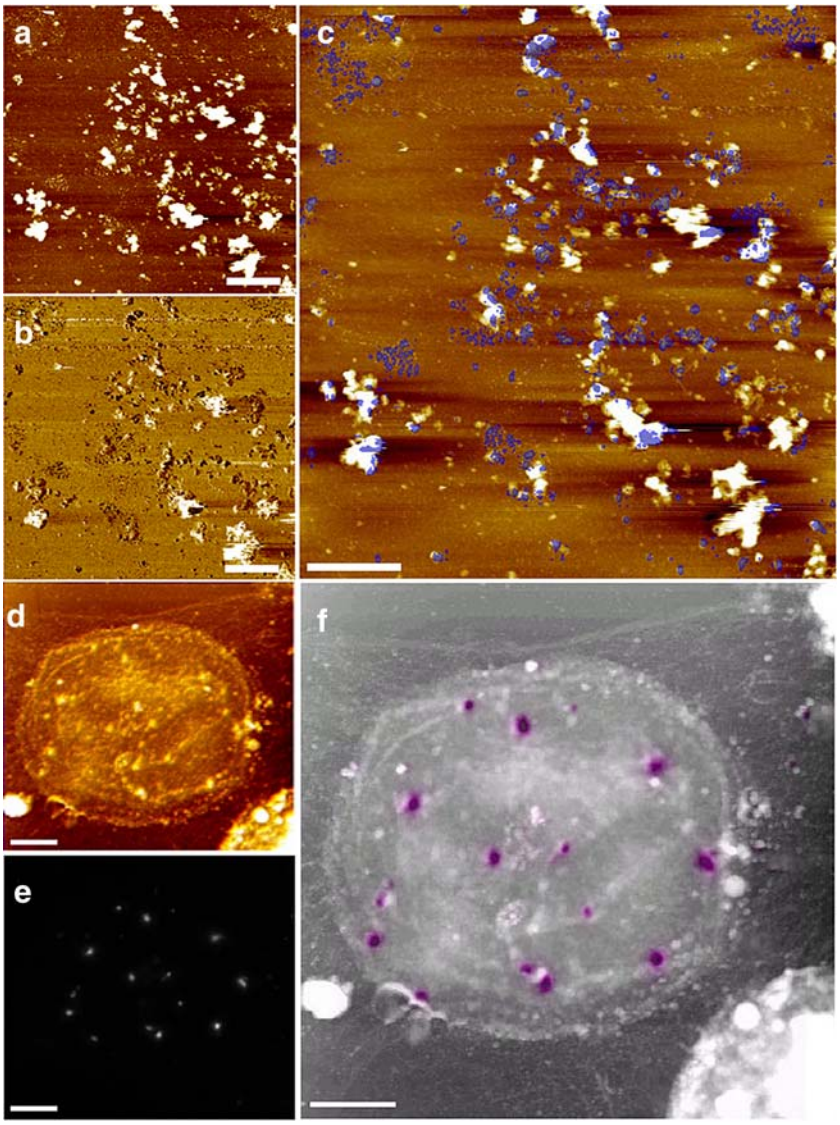

Fig. 4 Nuclear scaffold/matrix protein visualized by recognition imaging with Pico TREC™ (**a**–**c**) and hybrid imaging by AFM and fluorescence microscopy (**d**–**f**). The recognition signal and topographical signal were simultaneously recorded. Disrupted nuclei purified from HeLa cells were covalently attached on the amino-modified glass surface and imaged by TREC™-mode AFM with the anti-SP120 antibody-coupled cantilever. The topographical images (**a**) and corresponding recognition images (**b**) are shown. Scale bars= 1,000 nm. The merged image is shown in (**c**) where the recognition signals are in *blue*. The *dotted SP120 molecules* were recognized within the nuclear components (**c**). **d–f** Enhanced green fluorescent protein-fused PML was transiently expressed in HeLa cells on a cover glass. The cells were successively treated with detergent, high-salt solution and DNase I to expose nuclear matrix. The specimen was then observed by inverted fluorescence microscopy equipped with an AFM scanner on the stage. The AFM image (**d**) and the fluorescence image (**e**) are merged (**f**). The location of PML bodies can be mapped on the AFM image [*purple dots* in (**f**)]. Scale bars in (**a–c**) and (**d**–**f**) are 1 and 2 μm, respectively

to early telophase, these proteins formed intermediate structures called the pre-nucleolar bodies (PNBs) [131], and then, they are sequentially transported to the NORs, reflecting the roles of the proteins in rRNA processing and the ribosomal maturation process [132–134]. Inhibition of the cyclin-dependent kinase 1 (CDK1)–cyclin B activity during mitosis does not interfere with the reassembly of fibrillarin but does block the relocalization of one of the GC proteins, Nop52. Therefore, CDK1–cyclin B is partially responsible for the nucleolar reassembly, but the detailed mechanisms of the regulation of the entire event remain unknown [135].

Interaction between the nuclear envelope and chromatin

The nuclear envelope is a nanostructure that consists of the ONM, INM, NPC, and nuclear lamina (Fig. 6a). The structure of the nuclear envelope is critical for the control of the chromatin territory. The proteins in the INM, such as

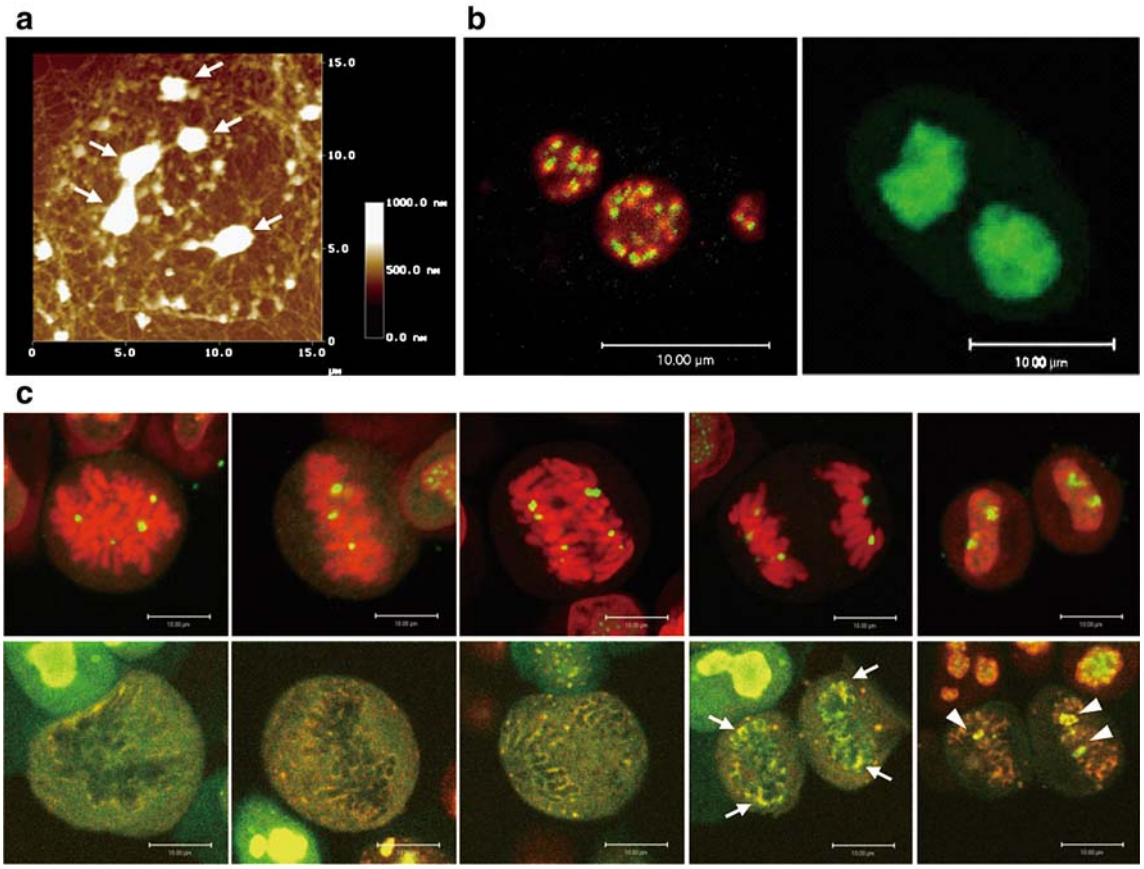

Fig. 5 Nucleolar structure and dynamics. **a** An AFM image of the nucleolus on the nuclear matrix. HeLa cells were sequentially treated with detergent, high-salt buffer, and DNase I. *Arrows* indicate nucleoli. **b** The subcellular localizations of the nucleolar proteins in interphase. *Left* double staining of the FC protein (our unpublished observation, *green*) and fibrillarin (DFC protein, *red*). *Right* localization of the nucleolin (GC protein). **c** The subcellular localizations of the nucleolar proteins during mitosis. *Upper panels* double staining of FC-localizing antigen (*green*) and DNA (*red*). *Lower panels* double staining of GFP-fibrillarin (*green*) and nucleolin (*red*). The PNBs are observed at telophase (*arrows*) and gradually targeted to the NORs (*arrowheads*). Scale bars=10 µm

LBR, are especially responsible for anchoring specific chromatin domains near the INM [25]. The nuclear lamina lies under the INM and guarantees the strength of the nucleus (Fig. 6a and b). EM observations have shown that the nuclear lamina is a mesh-like structure [136]. The major components of this structure are A- and B-type lamins. Both A- and B-type lamins form a dimer via their rod domains [137, 138]. The dimers further polymerize via the head–tail domains and form a para-crystal structure around 100 nm in length in vitro.

The structure of nuclear envelope is important, as the loss of it causes the disease termed nuclear envelopathy or laminopathy [138–140]. Then, the structural analysis of the nuclear envelope at nanoscale is needed.

Nuclear envelope in interphase

For decades, the nuclear envelope was recognized as a static structure in interphase. However, recent investigations with fluorescence recovery after photobleaching (FRAP) have revealed that most nuclear envelope proteins are mobile in the nuclear envelope except for the nuclear lamina and some of the nucleoporins [141–146]. The NPC functions as a gate to import and export substances into and out of the nucleus [147, 148]. It is a huge protein complex (Fig. 6b) with a molecular mass of 125 MDa, and it penetrates both the ONM and the INM [149, 150]. The NPC is composed of about 30 proteins named nucleoporins and forms an eightfold symmetrical structure [151–155]. The NPCs are likely to be newly synthesized and inserted into the nuclear envelope in the interphase cells. Interestingly, a huge NPC-free island can be observed during the early G1 phase in HeLa S3 cells, and this pore-free region disappears at the late G1 phase [156]. These results suggest that the NPCs are also under dynamic mobility control within the nuclear envelope.

The INM protein mobility seems to be restricted by the interaction between INM proteins and chromatin and/or nuclear lamina. Emerin and MAN1 are more mobile in the nuclear envelope in mouse embryonic fibroblasts lacking A-type lamin than in wild-type cells [157]. In contrast, a lack of A-type lamin does not affect the LBR mobility. The

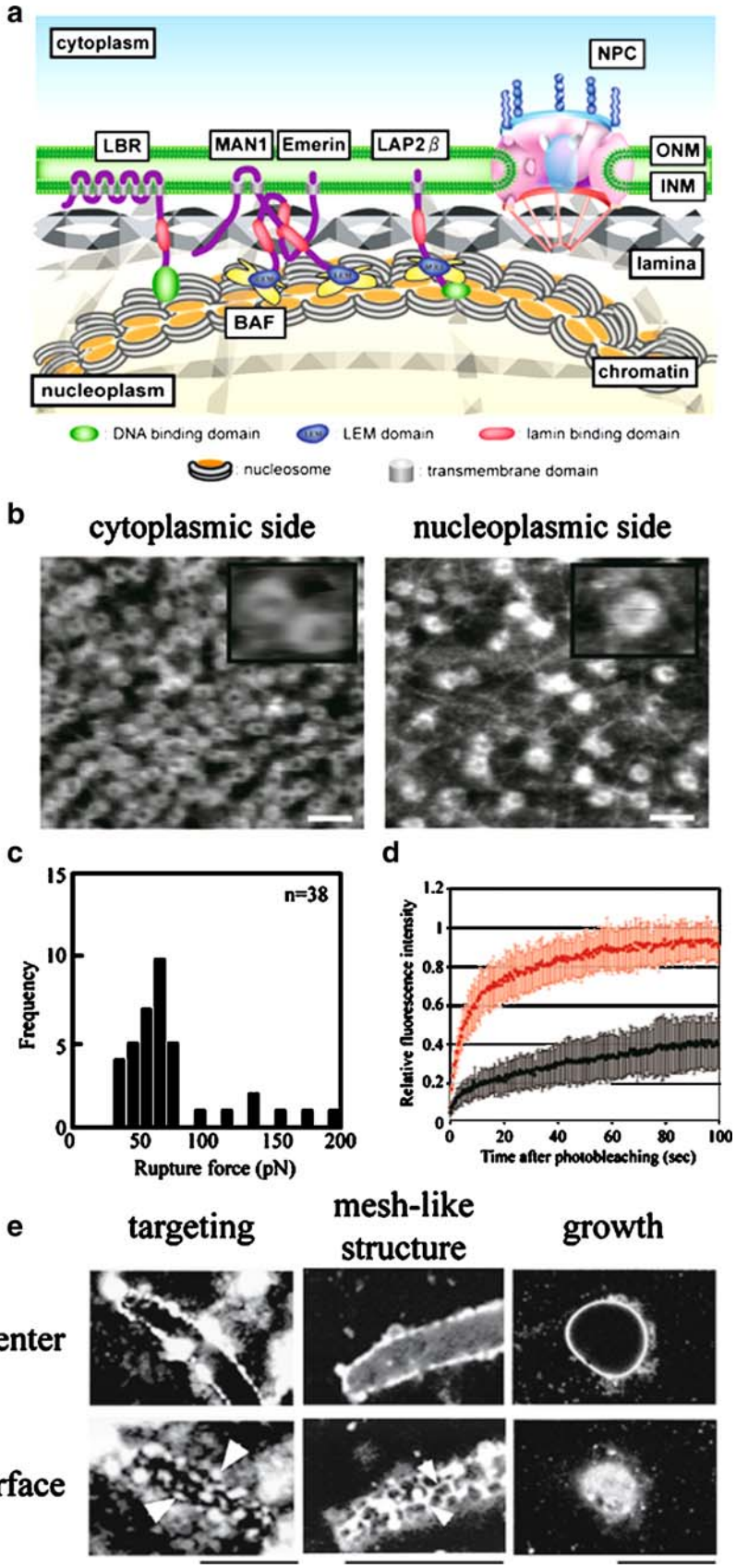

Fig. 6 The nuclear envelope during interphase (**a**–**d**) and mitosis (**e**). **a** Schematic illustration of the nuclear envelope. **b** AFM images of the nuclear envelope [164]. A germinal vesicle was isolated from a *Xenopus* oocyte. Its cytoplasmic (*left*) and nucleoplasmic face (*right*) were mechanically spread onto the mica and then imaged by AFM. Enlarged images are NPCs. Scale bars= 200 nm. **c** The rupture force measurement between LBR and chromatin. The GST-fused N-terminal region of LBR (amino acid region corresponding to 1–211) was expressed in *Escherichia coli* and purified by glutathione Sepharose beads. The purified GST-LBR was bound to an AFM cantilever via glutathione. Reconstituted chromatin was prepared from 26-kbp plasmid DNA and purified human histone octamer by the salt dialysis method and then bound to mica. The rupture force between LBR and reconstituted chromatin was measured, and a histogram of the rupture force is shown. **d** FRAP analysis of LBR mobility. GFP-tagged wild-type LBR (*black*) and a deletion mutant of the chromatin-binding region of LBR (Δ1–53, *red*) were transiently expressed in HeLa cells. The mobility of these proteins in the nuclear envelope was observed under LSM 510 META. **e** Nuclear membrane reassembly [165]. *Xenopus* egg crude extract was incubated with *Xenopus* sperm chromatin at 23°C. The chromatin-targeted membrane was stained with dihexyloxacarbocyanine iodide, and the central (*center*) and peripheral (*surface*) regions were observed by confocal microscopy. *Arrowheads* targeted nuclear membrane. Scale bars=10 μm

LBR seems to directly interact with chromatin [158]. Indeed, when the GST-fused N-terminal region of LBR (amino acid region 1–211, which contains the chromatin-binding domain) is attached to a glutathione-modified AFM cantilever, it exhibits a rupture force of ~50 pN against reconstituted chromatin (Fig. 6c). In live cells, the mobility of LBR in the nuclear envelope is much smaller than that of an N-terminal deletion mutant (Δ1–53) (Fig. 6d), suggesting that the interaction between the LBR and chromatin may be a key factor for chromatin attachment to the nuclear envelope.

Nuclear envelope at the mitotic phase

In many organisms, the nuclear envelope becomes invisible at the beginning of mitosis and reappears at the end of cell division (some organisms, such as most fungi, undergo closed mitosis, in which the nuclear envelope stays visible). At the onset of mitosis in animal cells, all of the nuclear envelope components (the INM, ONM, NPC, and nuclear lamina) are completely or partially broken down into small fragments or vesicles and disperse throughout the entire cell. After chromosome segregation in telophase, the nuclear envelope reassembles around the chromatin.

The molecular mechanism of nuclear envelope reassembly has been well studied in animal cells by using the *Xenopus* egg cell-free system (for details, see reviews [18, 19, 159]). Observations from fluorescence and EM have revealed that nuclear envelope reassembly occurs in three distinct steps: membrane vesicle targeting, membrane fusion, and growth (Fig. 6e) [160, 161]. At the end of mitosis, Ran, a small G protein, accumulates around the chromosome surface and forms a Ran-GTP gradient that causes the targeting of the nuclear membrane vesicles toward the chromosome surface. The INM proteins are also required in this step. Interestingly, *Xenopus* egg extracts contain two different vesicles, PV1 and PV2, which can be distinguished by ultracentrifugation [162]. These different vesicles are observed as ribosome-carrying 'rough' vesicles and ribosome-free 'smooth' vesicles [160]. The targeted membrane-vesicles fuse with each other, develop into a network with further vesicle fusion, and finally form a closed nuclear double-membrane around the entire area of nuclear chromatin. It seems that PV1 is a prerequisite for this step and that PV2 may be required for proper NPC assembly [162]. Finally, nuclear proteins (e.g., lamin) are imported into the growing nucleus through the newly synthesized NPCs, and the nucleus matures into a sphere-like structure.

The NPCs reassemble in parallel with the membrane fusion. However, as the depletion of the Nup 107–160 complex inhibits NPC formation but not nuclear membrane reassembly [163], the nuclear membrane reassembly is independent of the NPC formation. The structural aspects of the underlying mechanisms will hopefully be solved in the near future by using AFM.

Perspectives

The topographical imaging and visualization of biological specimens achieved by AFM have been extremely powerful tools for exploring basic concepts in fundamental biological processes. In this review, we have shown that AFM can be used to visualize the nanoscale structures of the inner nuclear architecture and higher-order folding of chromatin fibers. This approach has increased the understanding of how chromosomes are built up from DNA, histone, and other protein components. The physical properties of DNA were found to be critical for chromatin dynamics [16]. In contrast, the single-force measurement and recognition imaging have not yet been widely used. This is partly because a reliable procedure for attaching the protein of interest to the cantilever had not yet been established. We have developed new, efficient, and reliable methods for the attachment of antibodies and GST-fused proteins to the AFM cantilever [115], and we have used these methods to demonstrate a direct interaction between chromatin and INM proteins.

The field of nano-biology using scanning probe microscopy has been quickly progressing since the invention of AFM [33]. Just as the recent progress in genome research greatly benefited from the information obtained with bioinformatics, nano-biology will proceed to the next level by utilizing information from genome research and newly invented technology including recognition imaging [75] and fast-scanning AFM [47]. The elucidation of nuclear dynamics at the nanometer and piconewton levels will be accelerated. In the near future, it will also be possible to isolate individual processes in nuclear dynamics by fast-scanning AFM [44, 45]. Even beyond our specific objectives, recognition imaging, force measurement with specific probes, fast-scanning AFM, and other nanotechnologies are expected to be powerful tools in the various fields of biology.

Acknowledgements K.T. and S.H.Y. were supported by the grants, Priority Areas "Nuclear Dynamics" and "Cell Manipulation" from the Ministry of Education, Culture, Sports, Science and Technology of Japan, and a Grant-in-aid for Basic Research (A) and Basic Research for Young Scientists (A) from the Japan Society for the Promotion of Science (JSPS). K.H. and Y.H. were supported by a Grant-in-aid for Young Scientists (B) and a postdoctoral fellowship, respectively, from JSPS.

References

1. Nagata K, Takeyasu K (2007) Nuclear dynamics. Springer, Berlin

2. Kundu TK, Dasgupta D (2007) Chromatin and disease. Springer, Berlin
3. Kornberg RD (1974) Chromatin structure: a repeating unit of histones and DNA. Science 184:868–871
4. Kornberg RD, Thomas JO (1974) Chromatin structure; oligomers of the histones. Science 184:865–868
5. Wu C, Bingham PM, Livak KJ, Holmgren R, Elgin SC (1979) The chromatin structure of specific genes: I. Evidence for higher order domains of defined DNA sequence. Cell 16:797–806
6. Wu C, Wong YC, Elgin SC (1979) The chromatin structure of specific genes: II. Disruption of chromatin structure during gene activity. Cell 16:807–814
7. Richmond TJ, Davey CA (2003) The structure of DNA in the nucleosome core. Nature 423:145–150
8. Hizume K, Yoshimura SH, Takeyasu K (2005) Linker histone H1 per se can induce three-dimensional folding of chromatin fiber. Biochemistry 44:12978–12989
9. Leuba SH, Bustamante C, van Holde K, Zlatanova J (1998) Linker histone tails and N-tails of histone H3 are redundant: scanning force microscopy studies of reconstituted fibers. Biophys J 74:2830–2839
10. Leuba SH, Bustamante C, Zlatanova J, van Holde K (1998) Contributions of linker histones and histone H3 to chromatin structure: scanning force microscopy studies on trypsinized fibers. Biophys J 74:2823–2829
11. Thoma F, Koller T, Klug A (1979) Involvement of histone H1 in the organization of the nucleosome and of the salt-dependent superstructures of chromatin. J Cell Biol 83:403–427
12. Uchiyama S, Kobayashi S, Takata H, Ishihara T, Hori N, Higashi T, Hayashihara K, Sone T, Higo D, Nirasawa T, Takao T, Matsunaga S, Fukui K (2005) Proteome analysis of human metaphase chromosomes. J Biol Chem 280:16994–17004
13. Hizume K, Araki S, Yoshikawa K, Takeyasu K (2007) Topoisomerase II, scaffold component, promotes chromatin compaction in vitro in a linker-histone H1-dependent manner. Nucleic Acids Res 35:2787–2799
14. Swedlow JR, Hirano T (2003) The making of the mitotic chromosome: modern insights into classical questions. Mol Cell 11:557–569
15. Holmquist GP, Ashley T (2006) Chromosome organization and chromatin modification: influence on genome function and evolution.. Cytogenetic Genome Res 14::6–125
16. Kobori T, Hizume K, Ohniwa RL, Yoshimura SH, Takeyasu K (2007) Biochemical and biophysical basis of genome folding mechanism. In: Sanchez PC (ed) Progress in biopolymer reserarch. Nova Science Publishers, Inc.pp 107–135
17. Gant TM, Wilson KL (1997) Nuclear assembly. Annu Rev Cell Dev Biol 13:669–695
18. Hetzer MW, Walther TC, Mattaj IW (2005) Pushing the envelope: Structure, function, and dynamics of the nuclear periphery. Annu Rev Cell Dev Biol 21:347–380
19. Prunuske AJ, Ullman KS (2006) The nuclear envelope: form and reformation. Curr Opin Cell Biol 18:108–116
20. Schirmer EC, Gerace L (2005) The nuclear membrane proteome: extending the envelope. Trends Biochem Sci 30:551–558
21. Kawahire S, Tachibana T, Umemoto M, Yoneda Y, Imai N, Saito M, Ichimura T, Omata S, Horigome T (1996) Subcellular distribution and phosphorylation of the nuclear localization signal binding protein, NBP60. Exp Cell Res 222:385–394
22. Pyrpasopoulou A, Meier J, Maison C, Simos G, Georgatos SD (1996) The lamin B receptor (LBR) provides essential chromatin docking sites at the nuclear envelope. Embo J 15:7108–7119
23. Foisner R, Gerace L (1993) Integral membrane proteins of the nuclear envelope interact with lamins and chromosomes, and binding is modulated by mitotic phosphorylation. Cell 73:1267–1279
24. Yorifuji H, Tadano Y, Tsuchiya Y, Ogawa M, Goto K, Umetani A, Asaka Y, Arahata K (1997) Emerin, deficiency of which causes Emery–Dreifuss muscular dystrophy, is localized at the inner nuclear membrane. Neurogenetics 1:135–140
25. Lin F, Blake DL, Callebaut I, Skerjanc IS, Holmer L, McBurney MW, Paulin-Levasseur M, Worman HJ (2000) MAN1, an inner nuclear membrane protein that shares the LEM domain with lamina-associated polypeptide 2 and emerin. J Biol Chem 275:4840–4847
26. Gruenbaum Y, Margalit A, Goldman RD, Shumaker DK, Wilson KL (2005) The nuclear lamina comes of age. Nat Rev Mol Cell Biol 6:21–31
27. Tzur YB, Wilson KL, Gruenbaum Y (2006) SUN-domain proteins: 'Velcro' that links the nucleoskeleton to the cytoskeleton. Nat Rev Mol Cell Biol 7:782–788
28. Schirmer EC, Florens L, Guan T, Yates JR 3rd, Gerace L (2003) Nuclear membrane proteins with potential disease links found by subtractive proteomics. Science 301:1380–1382
29. Gruenbaum Y, Goldman RD, Meyuhas R, Mills E, Margalit A, Fridkin A, Dayani Y, Prokocimer M, Enosh A (2003) The nuclear lamina and its functions in the nucleus. Int Rev Cyt 226:1–62
30. Stein GS, Zaidi SK, Braastad CD, Montecino M, van Wijnen AJ, Choi JY, Stein JL, Lian JB, Javed A (2003) Functional architecture of the nucleus: organizing the regulatory machinery for gene expression, replication and repair. Trends Cell Biol 13:584–592
31. Cremer T, Cremer C (2001) Chromosome territories, nuclear architecture and gene regulation in mammalian cells. Nat Rev Genet 2:292–301
32. Tschochner H, Hurt E (2003) Pre-ribosomes on the road from the nucleolus to the cytoplasm. Trends Cell Biol 13:255–263
33. Binnig G, Quate CF, Gerber C (1986) Atomic force microscope. Phys Rev Lett 56:930–933
34. Hansma HG, Hoh JH (1994) Biomolecular imaging with the atomic force microscope.. Annu Rev Biophys Biomolecular Struct 23:115–139
35. Takeyasu K, Kim J, Ohniwa RL, Kobori T, Inose Y, Morikawa K, Ohta T, Ishihama A, Yoshimura SH (2004) Genome architecture studied by nanoscale imaging: analyses among bacterial phyla and their implication to eukaryotic genome folding. Cytogenet Genome Res 107:38–48
36. Hohmura KI, Itokazu Y, Yoshimura SH, Mizuguchi G, Masamura YS, Takeyasu K, Shiomi Y, Tsurimoto T, Nishijima H, Akita S, Nakayama Y (2000) Atomic force microscopy with carbon nanotube probe resolves the subunit organization of protein complexes. J Electron Microsc (Tokyo) 49:415–421
37. Akita S, Nishijima H, Nakayama Y, Tokumasu F, Takeyasu K (1999) Carbon nanotube tips for a scanning probe microscope: their fabrication and properties.. J Phys D: Appl Phys 32:1044–1048
38. Shiomi Y, Usukura J, Masamura Y, Takeyasu K, Nakayama Y, Obuse C, Yoshikawa H, Tsurimoto T (2000) ATP-dependent structural change of the eukaryotic clamp-loader protein, replication factor C. Proc Natl Acad Sci U S A 97:14127–14132
39. Ikai A, Afrin R (2003) Toward mechanical manipulations of cell membranes and membrane proteins using an atomic force microscope: an invited review. Cell Biochem Biophys 39:257–277
40. Ikai A, Afrin R, Sekiguchi H, Okajima T, Alam MT, Nishida S (2003) Nano-mechanical methods in biochemistry using atomic force microscopy. Curr Protein Pept Sci 4:181–193
41. Gamsjaeger R, Wimmer B, Kahr H, Tinazli A, Picuric S, Lata S, Tampe R, Maulet Y, Gruber HJ, Hinterdorfer P, Romanin C (2004) Oriented binding of the His6-tagged carboxyl-tail of the L-type Ca2+ channel alpha1-subunit to a new NTA-functionalized self-assembled monolayer. Langmuir 20:5885–5890
42. Yoshimura SH, Takahashi H, Otsuka S, Takeyasu K (2006) Development of glutathione-coupled cantilever for the single-

molecule force measurement by scanning force microscopy. FEBS Lett 580:3961–3965
43. Hinterdorfer P, Baumgartner W, Gruber HJ, Schilcher K, Schindler H (1996) Detection and localization of individual antibody-antigen recognition events by atomic force microscopy. Proc Natl Acad Sci U S A 93:3477–3481
44. Crampton N, Yokokawa M, Dryden DT, Edwardson JM, Rao DN, Takeyasu K, Yoshimura SH, Henderson RM (2007) Fast-scan atomic force microscopy reveals that the type III restriction enzyme EcoP15I is capable of DNA translocation and looping. Proc Natl Acad Sci U S A 104:12755–12760
45. Yokokawa M, Wada C, Ando T, Sakai N, Yagi A, Yoshimura SH, Takeyasu K (2006) Fast-scanning atomic force microscopy reveals the ATP/ADP-dependent conformational changes of GroEL. Embo J 25:4567–4576
46. Viani MB, Pietrasanta LI, Thompson JB, Chand A, Gebeshuber IC, Kindt JH, Richter M, Hansma HG, Hansma PK (2000) Probing protein–protein interactions in real time. Nat Struct Biol 7:644–647
47. Ando T, Kodera N, Takai E, Maruyama D, Saito K, Toda A (2001) A high-speed atomic force microscope for studying biological macromolecules. Proc Natl Acad Sci U S A 98:12468–12472
48. Yokokawa M, Yoshimura SH, Naito Y, Ando T, Yagi A, Sakai N, Takeyasu K (2006) Fast-scanning atomic force microscopy reveals the molecular mechanism of DNA cleavage by ApaI endonuclease. IEE Proc Nanobiotechnol 153:60–66
49. Bustamante C, Zuccheri G, Leuba SH, Yang G, Samori B (1997) Visualization and analysis of chromatin by scanning force microscopy. Methods (San Diego, Calif) 12:73–83
50. Hansma PK, Elings VB, Marti O, Bracker CE (1988) Scanning tunneling microscopy and atomic force microscopy: application to biology and technology. Science 242:209–216
51. Nettikadan S, Tokumasu F, Takeyasu K (1996) Quantitative analysis of the transcription factor AP2 binding to DNA by atomic force microscopy. Biochem Biophys Res Commun 226:645–649
52. Yoshimura SH, Ohniwa RL, Sato MH, Matsunaga F, Kobayashi G, Uga H, Wada C, Takeyasu K (2000) DNA phase transition promoted by replication initiator. Biochemistry 39:9139–9145
53. Ohta T, Nettikadan S, Tokumasu F, Ideno H, Abe Y, Kuroda M, Hayashi H, Takeyasu K (1996) Atomic force microscopy proposes a novel model for stem-loop structure that binds a heat shock protein in the *Staphylococcus aureus* HSP70 operon. Biochem Biophys Res Commun 226:730–734
54. Yoshimura SH, Yoshida C, Igarashi K, Takeyasu K (2000) Atomic force microscopy proposes a 'kiss and pull' mechanism for enhancer function. J Electron Microsc (Tokyo) 49:407–413
55. Sato MH, Ura K, Hohmura KI, Tokumasu F, Yoshimura SH, Hanaoka F, Takeyasu K (1999) Atomic force microscopy sees nucleosome positioning and histone H1-induced compaction in reconstituted chromatin. FEBS Lett 452:267–271
56. Fey EG, Krochmalnic G, Penman S (1986) The nonchromatin substructures of the nucleus: the ribonucleoprotein (RNP)-containing and RNP-depleted matrices analyzed by sequential fractionation and resinless section electron microscopy. J Cell Biol 102:1654–1665
57. Yoshimura SH, Kim J, Takeyasu K (2003) On-substrate lysis treatment combined with scanning probe microscopy revealed chromosome structures in eukaryotes and prokaryotes. J Electron Microsc (Tokyo) 52:415–423
58. Adolph KW, Kreisman LR, Kuehn RL (1986) Assembly of chromatin fibers into metaphase chromosomes analyzed by transmission electron microscopy and scanning electron microscopy. Biophys J 49:221–231
59. Tamayo J, Miles M (2000) Human chromosome structure studied by scanning force microscopy after an enzymatic digestion of the covering cell material. Ultramicroscopy 82:245–251
60. Belmont AS, Sedat JW, Agard DA (1987) A three-dimensional approach to mitotic chromosome structure: evidence for a complex hierarchical organization. J Cell Biol 105:77–92
61. Allen MJ, Lee C, Lee JDT, Pogany GC, Balooch M, Siekhaus WJ, Balhorn R (1993) Atomic force microscopy of mammalian sperm chromatin. Chromosoma 102:623–630
62. Ohniwa RL, Morikawa K, Kim J, Kobori T, Hizume K, Matsumi R, Atomi H, Imanaka T, Ohta T, Wada C, Yoshimura SH, Takeyasu K (2007) Atomic force microscopy dissects the hierarchy of genome architectures in eukaryote, prokaryote, and chloroplast. Microsc Microanal 13:3–12
63. Ohniwa RL, Morikawa K, Kim J, Ohta T, Ishihama A, Wada C, Takeyasu K (2006) Dynamic state of DNA topology is essential for genome condensation in bacteria. Embo J 25: 5591–5602
64. Alam MT, Yamada T, Carlsson U, Ikai A (2002) The importance of being knotted: effects of the C-terminal knot structure on enzymatic and mechanical properties of bovine carbonic anhydrase II. FEBS Lett 519:35–40
65. Baumgartner W, Hinterdorfer P, Ness W, Raab A, Vestweber D, Schindler H, Drenckhahn D (2000) Cadherin interaction probed by atomic force microscopy. Proc Natl Acad Sci U S A 97:4005–4010
66. Evans E, Leung A, Hammer D, Simon S (2001) Chemically distinct transition states govern rapid dissociation of single L-selectin bonds under force. Proc Natl Acad Sci U S A 98: 3784–3789
67. Hertadi R, Ikai A (2002) Unfolding mechanics of holo- and apocalmodulin studied by the atomic force microscope. Protein Sci 11:1532–1538
68. Neuert G, Albrecht C, Pamir E, Gaub HE (2006) Dynamic force spectroscopy of the digoxigenin-antibody complex. FEBS Lett 580:505–509
69. Sneddon IN (1965) The relation between load and penetration in the axisymmetric Boussinesq problem for a punch of arbitrary profile. Int J Engng Sci 3:47–57
70. Hofmann UG, Rotsch C, Parak WJ, Radmacher M (1997) Investigating the cytoskeleton of chicken cardiocytes with the atomic force microscope. J Struct Biol 119:84–91
71. Rotsch C, Radmacher M (2000) Drug-induced changes of cytoskeletal structure and mechanics in fibroblasts: an atomic force microscopy study. Biophys J 78:520–535
72. Nagayama M, Haga H, Kawabata K (2001) Drastic change of local stiffness distribution correlating to cell migration in living fibroblasts. Cell Motil Cytoskeleton 50:173–179
73. Nagayama M, Haga H, Takahashi M, Saitoh T, Kawabata K (2004) Contribution of cellular contractility to spatial and temporal variations in cellular stiffness. Exp Cell Res 300:396–405
74. Kienberger F, Kada G, Gruber HJ, Pastushenko VP, Riener C, Trieb M, Knaus H-G, Schindler H, Hinterdorfer P (2000) Recognition force spectroscopy studies of the NTA–His6 Bond. Single Mol 1:59–65
75. Stroh C, Wang H, Bash R, Ashcroft B, Nelson J, Gruber H, Lohr D, Lindsay SM, Hinterdorfer P (2004) Single-molecule recognition imaging microscopy. Proc Natl Acad Sci U S A 101: 12503–12507
76. Bash R, Wang H, Anderson C, Yodh J, Hager G, Lindsay SM, Lohr D (2006) AFM imaging of protein movements: histone H2A–H2B release during nucleosome remodeling. FEBS Lett 580:4757–4761
77. Baumann CG, Smith SB, Bloomfield VA, Bustamante C (1997) Ionic effects on the elasticity of single DNA molecules. Proc Natl Acad Sci U S A 94:6185–6190
78. Hagerman PJ (1981) Investigation of the flexibility of DNA using transient electric birefringence. Biopolymers 20:1503–1535

79. Shore D, Langowski J, Baldwin RL (1981) DNA flexibility studied by covalent closure of short fragments into circles. Proc Natl Acad Sci U S A 78:4833–4837
80. Wang MD, Yin H, Landick R, Gelles J, Block SM (1997) Stretching DNA with optical tweezers. Biophys J 72:1335–1346
81. Virstedt J, Berge T, Henderson RM, Waring MJ, Travers AA (2004) The influence of DNA stiffness upon nucleosome formation. J Struct Biol 148:66–85
82. Sakaue T, Yoshikawa K, Yoshimura SH, Takeyasu K (2001) Histone core slips along DNA and prefers positioning at the chain end. Phys Rev Lett 87:078105
83. Dame RT, Wyman C, Goosen N (2000) H-NS mediated compaction of DNA visualised by atomic force microscopy. Nucleic Acids Res 28:3504–3510
84. Kar S, Edgar R, Adhya S (2005) Nucleoid remodeling by an altered HU protein: reorganization of the transcription program. Proc Natl Acad Sci U S A 102:16397–16402
85. Margulies C, Kaguni JM (1998) The FIS protein fails to block the binding of DnaA protein to oriC, the *Escherichia coli* chromosomal origin. Nucleic Acids Res 26:5170–5175
86. Mizutani M, Ohta T, Watanabe H, Handa H, Hirose S (1991) Negative supercoiling of DNA facilitates an interaction between transcription factor IID and the fibroin gene promoter. Proc Natl Acad Sci U S A 88:718–722
87. Opel ML, Arfin SM, Hatfield GW (2001) The effects of DNA supercoiling on the expression of operons of the *ilv* regulon of *Escherichia coli* suggest a physiological rationale for divergently transcribed operons. Mol Microbiol 39:1109–1115
88. Schneider R, Lurz R, Luder G, Tolksdorf C, Travers A, Muskhelishvili G (2001) An architectural role of the *Escherichia coli* chromatin protein FIS in organising DNA. Nucleic Acids Res 29:5107–5114
89. Tabuchi H, Handa H, Hirose S (1993) Underwinding of DNA on binding of yeast TFIID to the TATA element. Biochem Biophys Res Commun 192:1432–1438
90. Hizume K, Yoshimura SH, Takeyasu K (2004) Atomic force microscopy demonstrates a critical role of DNA superhelicity in nucleosome dynamics. Cell Biochem Biophys 40:249–261
91. Nakai T, Hizume K, Yoshimura SH, Takeyasu K, Yoshikawa K (2005) Phase transition in reconstituted chromatin. Europhys Lett 69:1024–1030
92. Thoma F, Koller T (1977) Influence of histone H1 on chromatin structure. Cell 12:101–107
93. Ushiki T, Hoshi O, Iwai K, Kimura E, Shigeno M (2002) The structure of human metaphase chromosomes: its histological perspective and new horizons by atomic force microscopy. Arch Histol Cytol 65:377–390
94. Berrios M, Osheroff N, Fisher PA (1985) In situ localization of DNA topoisomerase II, a major polypeptide component of the *Drosophila* nuclear matrix fraction. Proc Natl Acad Sci U S A 82:4142–4146
95. Maeshima K, Laemmli UK (2003) A two-step scaffolding model for mitotic chromosome assembly. Dev Cell 4:467–480
96. Berger JM, Gamblin SJ, Harrison SC, Wang JC (1996) Structure and mechanism of DNA topoisomerase II. Nature 379:225–232
97. Nettikadan SR, Furbee CS, Muller MT, Takeyasu K (1998) Molecular structure of human topoisomerase II alpha revealed by atomic force microscopy. J Electron Microsc (Tokyo) 47:671–674
98. Wang JC (2002) Cellular roles of DNA topoisomerases: a molecular perspective. Nat Rev Mol Cell Biol 3:430–440
99. Uemura T, Ohkura H, Adachi Y, Morino K, Shiozaki K, Yanagida M (1987) DNA topoisomerase II is required for condensation and separation of mitotic chromosomes in *S. pombe*. Cell 50:917–925
100. Hirano T (2005) Condensins: organizing and segregating the genome. Curr Biol 15:R265–R275
101. Yoshimura SH, Hizume K, Murakami A, Sutani T, Takeyasu K, Yanagida M (2002) Condensin architecture and interaction with DNA: regulatory non-SMC subunits bind to the head of SMC heterodimer. Curr Biol 12:508–513
102. Jackson DA, Dickinson P, Cook PR (1990) The size of chromatin loops in HeLa cells. Embo J 9:567–571
103. Hancock R (2000) A new look at the nuclear matrix. Chromosoma 109:219–225
104. Tsutsui K, Okada S, Watarai S, Seki S, Yasuda T, Shohmori T (1993) Identification and characterization of a nuclear scaffold protein that binds the matrix attachment region DNA. J Biol Chem 268:12886–12894
105. Beck JS (1961) Variations in the morphological patterns of autoimmune nuclear fluorescence.1203–1205
106. Gall JG (2000) Cajal bodies: the first 100 years. Annu Rev Cell Dev Biol 16:273–300
107. Lamond AI, Spector DL (2003) Nuclear speckles: a model for nuclear organelles. Nat Rev Mol Cell Biol 4:605–612
108. Misteli T (2001) Protein dynamics: implications for nuclear architecture and gene expression. Science 291:843–847
109. Platani M, Goldberg I, Swedlow JR, Lamond AI (2000) In vivo analysis of Cajal body movement, separation, and joining in live human cells. J Cell Biol 151:1561–1574
110. Capco DG, Wan KM, Penman S (1982) The nuclear matrix: three-dimensional architecture and protein composition. Cell 29:847–858
111. Nickerson J (2001) Experimental observations of a nuclear matrix. J Cell Sci 114:463–474
112. Adolph KW (1980) Organization of chromosomes in HeLa cells: isolation of histone-depleted nuclei and nuclear scaffolds. J Cell Sci 42:291–304
113. Pederson T (2000) Half a century of "the nuclear matrix". Mol Biol Cell 11:799–805
114. Kiledjian M, Dreyfuss G (1992) Primary structure and binding activity of the hnRNP U protein: binding RNA through RGG box. Embo J 11:2655–2664
115. Takahashi H, Kawano S, Hirano Y, Tsutsui K, Tsutsui K, Yoshimura SH, Takeyasu K (2007) Efficient antibody-attachment to AFM Cantilever and Application to the Recognition Imaging. In Proceedings of the IX Linz Winter Workshop, Advances in single molecule research for biology and nanoscience
116. Sternsdorf T, Jensen K, Will H (1997) Evidence for covalent modification of the nuclear dot-associated proteins PML and Sp100 by PIC1/SUMO-1. J Cell Biol 139:1621–1634
117. Zhong S, Muller S, Ronchetti S, Freemont PS, Dejean A, Pandolfi PP (2000) Role of SUMO-1-modified PML in nuclear body formation. Blood 95:2748–2752
118. Gostissa M, Hofmann TG, Will H, Del Sal G (2003) Regulation of p53 functions: let's meet at the nuclear bodies. Curr Opin Cell Biol 15:351–357
119. Matsuzaki K, Minami T, Tojo M, Honda Y, Saitoh N, Nagahiro S, Saya H, Nakao M (2003) PML-nuclear bodies are involved in cellular serum response. Genes Cells 8:275–286
120. Zhong S, Salomoni P, Pandolfi PP (2000) The transcriptional role of PML and the nuclear body. Nat Cell Biol 2:E85–E90
121. Guo A, Salomoni P, Luo J, Shih A, Zhong S, Gu W, Pandolfi PP (2000) The function of PML in p53-dependent apoptosis. Nat Cell Biol 2:730–736
122. von Mikecz A, Zhang S, Montminy M, Tan EM, Hemmerich P (2000) CREB-binding protein (CBP)/p300 and RNA polymerase II colocalize in transcriptionally active domains in the nucleus. J Cell Biol 150:265–273
123. Andersen JS, Lyon CE, Fox AH, Leung AK, Lam YW, Steen H, Mann M, Lamond AI (2002) Directed proteomic analysis of the human nucleolus. Curr Biol 12:1–11
124. Scherl A, Coute Y, Deon C, Calle A, Kindbeiter K, Sanchez JC, Greco A, Hochstrasser D, Diaz JJ (2002) Functional proteomic analysis of human nucleolus. Mol Biol Cell 13:4100–4109
125. Jordan EG (1984) Nucleolar nomenclature. J Cell Sci 67:217–220

126. Scheer U, Thiry M, Goessens G (1993) Structure, function and assembly of the nucleolus. Trends Cell Biol 3:236–241
127. Junera HR, Masson C, Geraud G, Hernandez-Verdun D (1995) The three-dimensional organization of ribosomal genes and the architecture of the nucleoli vary with G1, S and G2 phases. J Cell Sci 108(Pt 11):3427–3441
128. Sato S, Yano H, Makimoto Y, Kaneta T, Sato Y (2005) Nucleolonema as a fundamental substructure of the nucleolus. J Plant Res 118:71–81
129. Roussel P, Andre C, Comai L, Hernandez-Verdun D (1996) The rDNA transcription machinery is assembled during mitosis in active NORs and absent in inactive NORs. J Cell Biol 133:235–246
130. Lawrence RJ, Earley K, Pontes O, Silva M, Chen ZJ, Neves N, Viegas W, Pikaard CS (2004) A concerted DNA methylation/histone methylation switch regulates rRNA gene dosage control and nucleolar dominance. Mol Cell 13:599–609
131. Hernandez-Verdun D (2006) Nucleolus: from structure to dynamics. Histochem Cell Biol 125:127–137
132. Savino TM, Gebrane-Younes J, De Mey J, Sibarita JB, Hernandez-Verdun D (2001) Nucleolar assembly of the rRNA processing machinery in living cells. J Cell Biol 153:1097–1110
133. Angelier N, Tramier M, Louvet E, Coppey-Moisan M, Savino TM, De Mey JR, Hernandez-Verdun D (2005) Tracking the interactions of rRNA processing proteins during nucleolar assembly in living cells. Mol Biol Cell 16:2862–2871
134. Leung AK, Gerlich D, Miller G, Lyon C, Lam YW, Lleres D, Daigle N, Zomerdijk J, Ellenberg J, Lamond AI (2004) Quantitative kinetic analysis of nucleolar breakdown and reassembly during mitosis in live human cells. J Cell Biol 166:787–800
135. Sirri V, Hernandez-Verdun D, Roussel P (2002) Cyclin-dependent kinases govern formation and maintenance of the nucleolus. J Cell Biol 156:969–981
136. Fawcett DW (1966) On the occurrence of a fibrous lamina on the inner aspect of the nuclear envelope in certain cells of vertebrates. Am J Anat 119:129–145
137. Hutchison CJ, Bridger JM, Cox LS, Kill IR (1994) Weaving a pattern from disparate threads: lamin function in nuclear assembly and DNA replication. J Cell Sci 107(Pt 12):3259–3269
138. De Sandre-Giovannoli A, Bernard R, Cau P, Navarro C, Amiel J, Boccaccio I, Lyonnet S, Stewart CL, Munnich A, Le Merrer M, Levy N (2003) Lamin a truncation in Hutchinson–Gilford progeria. Science 300:2055
139. Eriksson M, Brown WT, Gordon LB, Glynn MW, Singer J, Scott L, Erdos MR, Robbins CM, Moses TY, Berglund P, Dutra A, Pak E, Durkin S, Csoka AB, Boehnke M, Glover TW, Collins FS (2003) Recurrent de novo point mutations in lamin A cause Hutchinson–Gilford progeria syndrome. Nature 423:293–298
140. Hoffmann K, Dreger CK, Olins AL, Olins DE, Shultz LD, Lucke B, Karl H, Kaps R, Muller D, Vaya A, Aznar J, Ware RE, Sotelo Cruz N, Lindner TH, Herrmann H, Reis A, Sperling K (2002) Mutations in the gene encoding the lamin B receptor produce an altered nuclear morphology in granulocytes (Pelger–Huet anomaly). Nat Genet 31:410–414
141. Rabut G, Doye V, Ellenberg J (2004) Mapping the dynamic organization of the nuclear pore complex inside single living cells. Nat Cell Biol 6:1114–1121
142. Shimi T, Koujin T, Segura-Totten M, Wilson KL, Haraguchi T, Hiraoka Y (2004) Dynamic interaction between BAF and emerin revealed by FRAP, FLIP, and FRET analyses in living HeLa cells. J Struct Biol 147:31–41
143. Ellenberg J, Siggia ED, Moreira JE, Smith CL, Presley JF, Worman HJ, Lippincott-Schwartz J (1997) Nuclear membrane dynamics and reassembly in living cells: targeting of an inner nuclear membrane protein in interphase and mitosis. J Cell Biol 138:1193–1206
144. Daigle N, Beaudouin J, Hartnell L, Imreh G, Hallberg E, Lippincott-Schwartz J, Ellenberg J (2001) Nuclear pore complexes form immobile networks and have a very low turnover in live mammalian cells. J Cell Biol 154:71–84
145. Ostlund C, Ellenberg J, Hallberg E, Lippincott-Schwartz J, Worman HJ (1999) Intracellular trafficking of emerin, the Emery–Dreifuss muscular dystrophy protein. J Cell Sci 112(Pt 11):1709–1719
146. Wu W, Lin F, Worman HJ (2002) Intracellular trafficking of MAN1, an integral protein of the nuclear envelope inner membrane. J Cell Sci 115:1361–1371
147. Conti E, Muller CW, Stewart M (2006) Karyopherin flexibility in nucleocytoplasmic transport. Curr Opin Struct Biol 16:237–244
148. Imamoto N (2000) Diversity in nucleocytoplasmic transport pathways. Cell Struct Funct 25:207–216
149. Rout MP, Aitchison JD, Suprapto A, Hjertaas K, Zhao Y, Chait BT (2000) The yeast nuclear pore complex: composition, architecture, and transport mechanism. J Cell Biol 148:635–651
150. Rout MP, Aitchison JD (2001) The nuclear pore complex as a transport machine. J Biol Chem 276:16593–16596
151. Cronshaw JM, Krutchinsky AN, Zhang W, Chait BT, Matunis MJ (2002) Proteomic analysis of the mammalian nuclear pore complex. J Cell Biol 158:915–927
152. Oberleithner H (1999) Aldosterone and nuclear signaling in kidney. Steroids 64:42–50
153. Oberleithner H, Brinckmann E, Schwab A, Krohne G (1994) Imaging nuclear-pores of aldosterone-sensitive kidney-cells by atomic-force microscopy. Proc Natl Acad Sci U S A 91:9784–9788
154. Oberleithner H, Schafer C, Shahin V, Schlune A, Schillers H, Reinhardt J (2001) Nuclear plug harvesting using atomic force microscopy. Single Mol 2:117–120
155. Oberleithner H, Schillers H, Wilhelmi M, Butzke D, Danker T (2000) Nuclear pores collapse in response to CO2 imaged with atomic force microscopy. Pflugers Archiv 439:251–255
156. Maeshima K, Yahata K, Sasaki Y, Nakatomi R, Tachibana T, Hashikawa T, Imamoto F, Imamoto N (2006) Cell-cycle-dependent dynamics of nuclear pores: pore-free islands and lamins. J Cell Sci 119:4442–4451
157. Ostlund C, Sullivan T, Stewart CL, Worman HJ (2006) Dependence of diffusional mobility of integral inner nuclear membrane proteins on A-type lamins. Biochemistry 45:1374–1382
158. Ye Q, Worman HJ (1994) Primary structure analysis and lamin B and DNA binding of human LBR, an integral protein of the nuclear envelope inner membrane. J Biol Chem 269:11306–11311
159. Margalit A, Vlcek S, Gruenbaum Y, Foisner R (2005) Breaking and making of the nuclear envelope. J Cell Biochem 95:454–465
160. Wiese C, Goldberg MW, Allen TD, Wilson KL (1997) Nuclear envelope assembly in Xenopus extracts visualized by scanning EM reveals a transport-dependent 'envelope smoothing' event. J Cell Sci 110(Pt 13):1489–1502
161. Hetzer M, Meyer HH, Walther TC, Bilbao-Cortes D, Warren G, Mattaj IW (2001) Distinct AAA-ATPase p97 complexes function in discrete steps of nuclear assembly. Nat Cell Biol 3:1086–1091
162. Sasagawa S, Yamamoto A, Ichimura T, Omata S, Horigome T (1999) In vitro nuclear assembly with affinity-purified nuclear envelope precursor vesicle fractions, PV1 and PV2. Eur J Cell Biol 78:593–600
163. Walther TC, Alves A, Pickersgill H, Loiodice I, Hetzer M, Galy V, Hulsmann BB, Kocher T, Wilm M, Allen T, Mattaj IW, Doye V (2003) The conserved Nup107–160 complex is critical for nuclear pore complex assembly. Cell 113:195–206
164. Otsuka S, Takahashi H, Takeyasu K, Yoshimura SH (2006) Molecular mechanism of protein transport across nuclear membrane. Recent Res Devel Biophys 5:245–256
165. Nakagawa T, Hirano Y, Inomata A, Yokota S, Miyachi K, Kaneda M, Umeda M, Furukawa K, Omata S, Horigome T (2003) Participation of a fusogenic protein, glyceraldehyde-3-phosphate dehydrogenase, in nuclear membrane assembly. J Biol Chem 278:20395–20404